



Discriminating Sleep From Freezing With Cortical Spindle Oscillations

Marco N. Pompili^{1*} and Ralitsa Todorova^{2*}

¹ Aix Marseille University, INSERM, Institut de Neurosciences des Systèmes (INS), Marseille, France, ² Department of Neurobiology and Behavior, Cornell University, Ithaca, NY, United States

In-vivo longitudinal recordings require reliable means to automatically discriminate between distinct behavioral states, in particular between awake and sleep epochs. The typical approach is to use some measure of motor activity together with extracellular electrophysiological signals, namely the relative contribution of theta and delta frequency bands to the Local Field Potential (LFP). However, these bands can partially overlap with oscillations characterizing other behaviors such as the 4 Hz accompanying rodent freezing. Here, we first demonstrate how standard methods fail to discriminate between sleep and freezing in protocols where both behaviors are observed. Then, as an alternative, we propose to use the smoothed cortical spindle power to detect sleep epochs. Finally, we show the effectiveness of this method in discriminating between sleep and freezing in our recordings.

Keywords: sleep spindles, behavioral state classification, freezing, sleep, cortical oscillations, local field potential oscillations

OPEN ACCESS

Edited by:

Gabrielle Girardeau,
INSERM U839 Institut du Fer à Moulin
(IFM), France

Reviewed by:

Thomas C. Watson,
University of Edinburgh,
United Kingdom
Ross Purple,
University of Bristol, United Kingdom

*Correspondence:

Marco N. Pompili
marco.pompili@normalesup.org
Ralitsa Todorova
rt428@cornell.edu

Received: 26 September 2021

Accepted: 31 January 2022

Published: 24 March 2022

Citation:

Pompili MN and Todorova R (2022)
Discriminating Sleep From Freezing
With Cortical Spindle Oscillations.
Front. Neural Circuits 16:783768.
doi: 10.3389/fncir.2022.783768

1. INTRODUCTION

One of the main ambitions of systems neuroscience is to understand the relationship between the activity of the nervous system and animal behavior. To this end, a fruitful approach is to record neural activity as animals perform specific tasks as well as during natural behavior. Indeed, monitoring brain activity across a wide range of training-dependent and spontaneous behavioral states is crucial in the study of potential mappings between neural activity and behavior (Krakauer et al., 2017). Moreover, contrasting the neurophysiology of active vs. inactive states (such as rest), helps disentangle the neural activity underpinning cognitive functions such as learning from those controlling motor behavior and perception. In particular, the neurophysiology of sleep examines endogenous activity taking place when the brain is disengaged from the external world and self-organized computation emerges (Buzsáki et al., 2014).

In electrophysiological studies, neural activity can be recorded for many hours, and in some cases days or weeks, across many behavioral states (e.g., Wilson and McNaughton, 1994; Hirase et al., 2001; Lin et al., 2006; Benchenane et al., 2010; Hengen et al., 2016; Dhawale et al., 2017; Girardeau et al., 2017; Chung et al., 2019; Todorova and Zugaro, 2019). Matching specific neural processes to particular behaviors requires reliable automated means to distinguish between different behavioral states, such as wakefulness vs. sleep, but also between rapid eye movement (REM) sleep and non-REM sleep, also known as slow-wave sleep (SWS).

State of the art automated brain state scoring techniques rely on motor activity as well as neural recordings, taking advantage of the fact that active awake behavior and REM are characterized by oscillations in the theta frequency band (7–8.5 Hz), while SWS is dominated by slower rhythms in the delta range (1–4 Hz). The most common approach for classifying sleep stages consists of sampling animal movement (using video recordings, inertial sensors, or electromyography) to

detect immobility periods, and then dividing the resulting epochs into REM and SWS based on the relative power of theta vs. delta oscillations in the electroencephalography or local field potential (LFP) recordings. This technique has been used for more than 40 years (Gottesmann et al., 1971; Kohn et al., 1974; Johns et al., 1977) and is still very popular today (e.g., Todorova and Zugaro, 2019; Sosa et al., 2020; Wang et al., 2020; Tingley et al., 2021).

A limitation of this approach is the assumption that all immobility corresponds to rest, uniquely composed of its sub-states: quiet wakefulness, SWS, and REM. However, certain behavioral paradigms may involve immobility which should not be equated to resting. In particular, immobility is also the main feature of freezing behavior (Blanchard and Blanchard, 1969), a widely used index of fear typically employed to probe for learning in fear conditioning (Fanselow and Poulos, 2005), a very popular paradigm in rodent behavioral research. This presents a problem for studies addressing the role of sleep in emotional regulation and fear memory consolidation, a research focus likely to become more and more popular since sleep neurophysiology is finally crossing paths with the investigation of emotional learning (Trouche et al., 2020).

In order to correctly discriminate between sleep and freezing in a behavioral protocol involving both behaviors, we developed a method based on spindle oscillations in cortical recordings. Spindle oscillations are characteristic of SWS (Steriade et al., 1993; Fernandez and Lüthi, 2020), which constitutes 90% or rodents sleep (Brankack et al., 2010). Here, after illustrating how standard approaches, by construction, cannot discriminate between freezing and sleep/rest states, we show how these can be disentangled by the smoothed spindle power. Finally, we validate that this approach was effective in detecting sleep and freezing epochs interspersed in a fear conditioning and extinction paradigm. The algorithm we propose requires solely the LFP from a single neocortical channel and a readout of the animal motor activity and is therefore a simple and effective solution to determine behavioral states in freely moving animal recordings.

2. RESULTS

2.1. Standard Approach Fails to Distinguish Sleep From Freezing

As a case study, we analyzed data recorded from rats performing both freezing and sleeping behaviors. The rats underwent a multi-day fear conditioning and extinction protocol, and rest sessions were recorded in a familiar non-anxiogenic environment before and after each training session (Figure 1A).

We first used standard methods to detect freezing and sleep. Freezing is typically defined as all immobility periods longer than a particular threshold (0.5–2 s; e.g., Bagur et al., 2018; Moberly et al., 2018; Gründemann et al., 2019; Jercog et al., 2021; Ressler et al., 2021). Nonetheless, standard sleep-scoring algorithms assume that all such immobility corresponds to rest states. Therefore, these techniques label most immobility periods as both sleep and freezing. Indeed, while in some cases immobility periods correspond to sleep

(see the left part of Figure 1B; Supplementary Video 1), a freezing period may also last for long periods of time (right part of Figure 1B; Supplementary Video 2). This makes the standard approach to sleep detection unsuitable for data involving freezing.

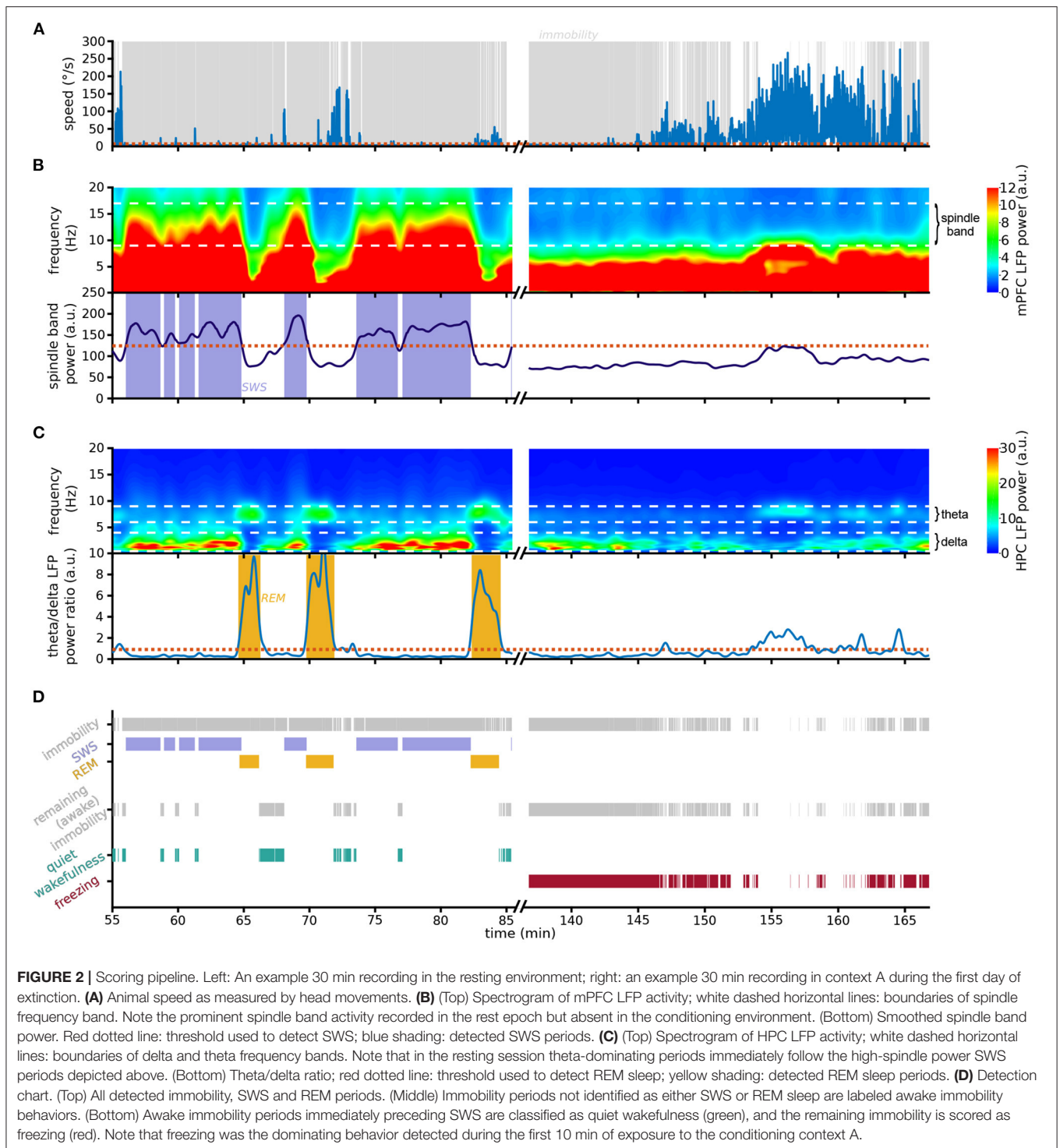
Our recordings included the local field potential (LFP) from the hippocampus (HPC) and medial prefrontal cortex (mPFC). As expected, theta and delta oscillations displayed a marked difference between REM and SWS epochs (Figure 2C). However, the theta/delta ratio did not help separate SWS from freezing, because in both of these epochs delta power dominated over theta power (Figure 1B). This is likely due to the overlap between the delta frequency band and the frequency band of the respiratory-driven cortical oscillation around 4 Hz associated with freezing (Ciatipis et al., 2014; Karalis et al., 2016; Lockmann et al., 2016; Biskamp et al., 2017; Moberly et al., 2018; Bagur et al., 2021; Karalis and Sirota, 2022). On the other hand, power in the spindle band (9–17 Hz) was high in sleep epochs and low in freezing (Figure 1B), suggesting that spindle power may be an exclusive marker for SWS.

2.2. Smoothed Cortical Spindle Power to Detect SWS

To develop a method to separate freezing and sleep, we took advantage of the lack of overlap between the spindle frequency and the slower 4 Hz oscillation associated with freezing. On the fine timescale, spindle power increases particularly during individual spindles, which are distinct thalamocortical events occurring in SWS. However, spindle events are common in SWS, and therefore the *smoothed* spindle power is relatively constant as it joins multiple spindle events (Supplementary Figure 1). Indeed, the smoothed spindle power during immobility periods follows a bimodal distribution (Supplementary Figure 2), allowing the separation between SWS and non-SWS immobility periods as they are characterized by high and low smoothed spindle power, respectively.

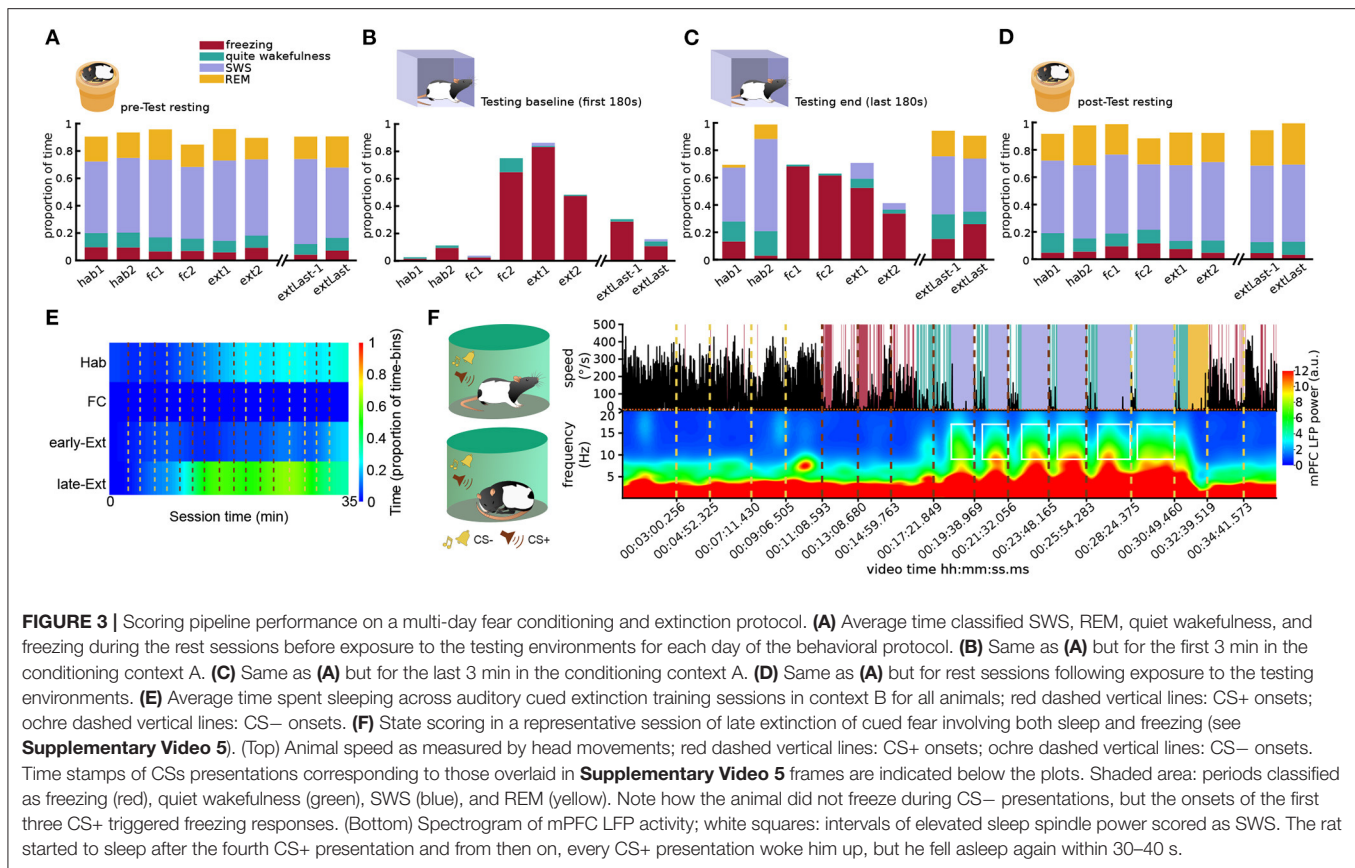
The pipeline we developed (see Section 4 for details) starts by detecting all periods of immobility (Figure 2A). We then classify immobility periods with high spindle power as SWS (Figure 2B). Since REM periods do not occur in isolation but are nested within SWS cycles (McCarley, 2007), we label as REM sleep those epochs where HPC theta power is higher than HPC delta power, on the condition that they closely follow SWS (Figure 2C). In the absence of HPC recordings the algorithm can detect REM using the theta/delta ratio of the cortical LFP used to detect SWS (Supplementary Figure 3).

The remaining immobility periods are considered non-sleep immobility states (Figure 2D). These include the periods of quiet wakefulness prior to falling asleep, which must be disentangled from freezing. We therefore classify these SWS-preceding immobility periods as quiet wakefulness epochs, and the remaining immobility is labeled as freezing (Figure 2D). Contrary to a compounded use of the standard approaches for sleep and freezing detection, this method is designed to guarantee



observe both of these behaviors in the same sessions, which can sometimes involve abrupt transitions between states. To test the performance of our method in such a scenario, we analyzed the moments when an animal slept when a CS+ was being presented in cued fear extinction sessions. Indeed, the unanticipated presentations of a strong sound can

wake up the sleeping animal. In the example in **Figure 3F; Supplementary Video 5**, the first couple of CS+ presentations induced freezing behavior, which was detected by our method because smoothed spindle power remained low during these immobility periods. After some minutes, the animal fell asleep, which was accompanied by increased smoothed spindle power.



Each subsequent CS presentation briefly woke the animal up, resulting in sleep-wake-sleep transitions detected by our method. The smoothed spindle power can therefore serve as a precise tag for SWS.

Finally, while ground truth data for the internal state of the animal is impossible to obtain, we compared the results of the algorithm to the scoring by an expert observer, blind to the algorithm results, who manually labeled 2 s video snippets ($n = 600$) classified as either freezing or sleep by the algorithm across five recording sessions from three different animals. The freezing vs. sleep separation by this manual scoring agreed with the algorithm classification 92% of the time.

3. DISCUSSION

Discriminating between freezing and resting states can be critical in longitudinal recordings of emotional behavior. However, traditionally, these behaviors have been studied separately, and standard scoring methods using immobility and theta/delta ratio cannot disambiguate between them. Unlike delta band power, the smoothed spindle power in cortical LFP recordings can correctly identify SWS epochs and separate them from freezing. The remaining immobility periods can be scored as REM sleep, quiet wakefulness, or freezing, depending on the theta/delta ratio and their timing to detected SWS epochs. We applied

this approach to recordings of rats involving both freezing and sleep as part of a fear conditioning and extinction protocol, and our results are consistent with correct scoring of freezing and sleep states.

The key advantage of the smoothed spindle power is that while it is high in SWS, it remains low during freezing. Basing the SWS detection on this signal alone thus avoids confounding SWS and freezing, when other signals such as delta power can respond strongly to both behaviors due to the overlap between the delta band and the 4 Hz oscillation (2–5 Hz respiratory-driven rhythmic activity; Moberly et al., 2018). While the spindle band power is used by many sleep classification algorithms (e.g., Gottesmann et al., 1977; Louis et al., 2004; Liang et al., 2012; Supratak et al., 2017), its contribution is often secondary to slow oscillations in the delta band. Therefore, these algorithms can be used to score sleep stages only after freezing has already been excluded, but they were not designed to separate between sleep and freezing, especially given their assumption that all immobility corresponds to resting states.

Recently, Bagur et al. (2018) showed that sleeping and freezing states can be disambiguated using oscillations recorded in the olfactory bulb. This is a powerful method which resolves the sleeping/freezing ambiguity. Using the neocortical smoothed spindle power as proposed here can be an alternative in the absence of such recordings from the olfactory bulb.

Here, we introduced a technique to detect SWS periods based solely upon the smoothed spindle band oscillatory activity and we demonstrated its effectiveness in our data. To our knowledge, this is the only automated approach discriminating between freezing and resting immobility in the absence of olfactory bulb recordings. Our algorithm is straightforward to implement as it only requires recording from a single neocortical electrode, and it could be of use for future systems neuroscience research involving both fear and rest behavioral states. Moreover, the lack of overlap between the spindle band and breathing frequencies observed in immobility (Herent et al., 2020) can help separate sleep from other awake behaviors beyond freezing, permitting the smoothed spindle power to serve as a simple method to detect SWS in general.

4. MATERIALS AND METHODS

4.1. Recording of Neural Activity During a Multi-Day Fear Conditioning and Extinction Training Protocol and Peri-Training Rest

4.1.1. Animals

Five male Long-Evans rats (350–400 g at the time of the surgery, 2–5 months old) were housed individually in monitored conditions (21°C and 45% humidity) and maintained on a 12 h light–12 h dark cycle. In order to avoid obesity, feeding was restricted to 13–16 g chow per day, with water available *ad libitum*. To habituate the rats to human manipulation, they were handled each workday. All experiments conformed to the approved protocols and regulations of the local ethics committee and the French ministry of agriculture and the French ministry of higher education and research.

4.1.2. Surgery

Rats were deeply anesthetized using a ketamine-xylazine mixture (Imalgene and Rompun, 180 and 10 mg/kg, respectively) and anesthesia was maintained with isoflurane (0.1–1.5% in oxygen). Analgesia was assured by subcutaneous injection of buprenorphine (Buprecaire, 0.025 mg/kg) and meloxicam (Metacam, 3 mg/kg). The animals were implanted bilaterally with a custom built microdrive with 24–42 bundles of independently movable twisted electrodes (12 μ m tungsten wires twisted in groups of either six or eight wires and gold-plated to 200 k Ω) 0.5 mm above the target brain regions. Electrode bundle placement varied between rats. Nevertheless, in all animals there were electrodes implanted in the medial prefrontal cortex (stereotaxic coordinates: \pm 0.3–0.6 mm mediolateral and +2.5–4.8 mm anteroposterior from bregma) and dorsal hippocampus (\pm 3.8–5 mm mediolateral and –5 mm anteroposterior from bregma). During recovery after surgery (minimum 7 days), the rats received antibiotic (Marbofloxacin, 2 mg/kg) and analgesic (Meloxicam, 3 mg/kg) treatments via subcutaneous injections, and were provided with food and water *ad libitum*. The recording

electrodes were then progressively lowered until they reached their targets.

4.1.3. Behavioral Apparatus

After full recovery, rats were exposed to two testing environments (context A and context B), and one resting environment. Context A was a cubicle conditioning chamber (40 \times 40 \times 40 cm) with gray plexiglass walls lined with ribbed black rubber sheets and a floor composed of nineteen stainless steel rods [0.48 cm diameter with 1.6 cm spacing connected to a scrambled shock generator (ENV-414S, Med Associates, USA)]. It was mildly scented daily with mint-perfumed cleaning solution (Simple Green, Sunshine Makers). Context B was a stadium-shaped PVC enclosure (30 cm side and 15 cm radius) with a black wooden floor and walls lined with light brown pieces of rope rug. It was mildly scented daily with a vanilla extract solution. The resting environment was a cloth-lined plastic flowerpot (30 cm upper diameter, 20 cm lower diameter, 25 cm high). Auditory stimuli (conditioned stimuli, CSs) were delivered in either of the two testing environments via a custom-made electronic system. The stimuli were white noise (CS+) or 8 kHz pure tone (CS–) 250 ms long pips repeated at 1 Hz for the duration of 20 s at 80 dB.

4.1.4. Behavioral Protocol

Habituation took place on days 1 and 2. On day 1, CSs were presented in one context and on day 2 they were presented in the other (context order presentation was switched every day and was counterbalanced across animals), habituating the animals to the stimuli. On days 3 and 4, the animals were fear conditioned in context A, where CS+ presentations were coupled with foot shocks (1 s, 0.6 mA, co-terminating with CS+ presentations). Extinction training began on day 5, with CS presentations in context B and context exposure (no CS presentations) in context A. Extinction training was repeated every day until the rat was seen sleeping throughout CS+ presentations.

Every day of the experimental protocol consisted of one 35 min session in each context. When introduced in the contexts the animals were either presented with the auditory CSs (after a baseline period of 3 min, the animals were presented to 16 CSs, 8 CS+, and 8 CS–, separated by inter-trial intervals of random duration, range 120–240 s) or received no auditory stimuli (context exposure sessions). During habituation and fear conditioning, CS+ and CS– were presented in pseudorandom order (no more than 2 consecutive presentations of the same-type CS), while in extinction training, 4 CS– were presented first, followed by 8 CS+ and then 4 CS–. Before and after each session the animals were left undisturbed for at least 2 h in the resting environment to record sleep activity.

4.1.5. Data Acquisition and Processing

An inertial measurement unit (IMU, non wireless version of the one described in Pasquet et al., 2016) recorded 3D angular velocity and linear acceleration of the animals' heads (sampled at 300 Hz). Animal behavior was also recorded by lateral video

cameras (50 Hz sampling rate) in contexts A and B (acA25000, Basler). Brain activity was recorded wideband at 20,000 Hz using a KJE-1001 data acquisition system (Amplipex, Szeged, Hungary). Neurophysiological and behavioral data were explored with NeuroScope (Hazan et al., 2006). LFPs were derived from wideband signals by downsampling all channels to 1,250 Hz. At the end of the experiments, recording sites were marked with small electrolytic lesions ($\sim 20 \mu\text{A}$ for 20 s, one lesion per bundle). After a delay of at least 3 days to permit glial scarring, rats were deeply anesthetized with a lethal dose of pentobarbital and intracardially perfused with saline (0.9%) followed by paraformaldehyde (4%). Coronal slices ($35 \mu\text{m}$) were stained with cresyl-violet and imaged with conventional transmission light microscopy (**Supplementary Figure 5**). Recording sites were reconstructed by comparing the images with the stereotaxic atlas of Paxinos and Watson (2013).

4.2. Data Analysis and Statistics

Data were analyzed using FMAToolbox (<http://fmatoolbox.sourceforge.net>), Chronux (<http://chronux.org/>), and custom written programs in Matlab (MathWorks, Natick, MA).

4.2.1. Scoring of Behavioral States With Standard Approaches

In order to compare our proposed approach with standard sleep and freezing detection protocols, we performed standard behavioral scoring as follows. Automatic detection of immobility was performed by applying a threshold detection routine to the angular speed calculated from gyroscope data as we described previously (Pasquet et al., 2016).

4.2.1.1. Freezing Detection

Typically, the minimum duration of immobility to be classified as freezing ranges between 0.5 and 2 s, and brief movements of 0.1–0.2 s are ignored (e.g., Courtin et al., 2014; Jercog et al., 2021). We therefore defined freezing as moments where the animals remained immobile for more than 1.5 s, ignoring brief movements of < 0.2 s.

4.2.1.2. Sleep Detection

To identify sleep stages (NREM and REM), LFP data was visualized using Neuroscope (Hazan et al., 2006) and a hippocampal channel with clear theta oscillations during exploration was identified. The signal from this channel was filtered in the theta (6–9 Hz) and delta (0.5–4 Hz) bands. Typically, only periods longer than 30–120 s are retained as sleep and periods around brief movements of 0.5–1 s are merged together (e.g., Drieu et al., 2018; Todorova and Zugaro, 2019). Therefore, here, only the periods of immobility lasting longer than 60 s were considered, and brief movements shorter than 1 s were ignored. The time bins of theta/delta ratio of these periods were clustered in two groups with k-means.

4.2.2. Scoring of Behavioral States With Spindle Power

4.2.2.1. Slow Wave Sleep Detection

Immobility was detected as above. LFP data was visualized using Neuroscope (Hazan et al., 2006) and a channel with distinct

spindles during sleep (mPFC) was selected. The LFP signal was filtered in the spindle band (9–17 Hz), and the instantaneous amplitude was estimated using the Hilbert transform. This amplitude was then smoothed (Gaussian window of 14 s), and immobility periods where the smoothed amplitude exceeded a k-means identified threshold (**Supplementary Figure 2**) were classified as SWS. The minimum duration allowed for sleep bouts and the maximum duration of small movements are parameters that users are free to select. For the results presented here these parameters were set to 30 and 1 s, respectively.

4.2.2.2. REM Sleep Detection

The remaining immobility periods where the ratio between the theta (6–9 Hz) and delta (0.5–4 Hz) power of the HPC LFP signal exceeded 1 and followed a SWS period were classified as REM. The maximum delay by which REM periods can follow SWS is a parameter set by the user. However, since SWS to REM transitions are known to last up to 30 s (Datta and Hobson, 2000), we recommend allowing for at least 30 s.

In the absence of hippocampal LFP the algorithm can detect REM periods using the theta/delta ratio of the cortical LFP used to detect SWS, with the following adjustments. First, the cortical theta/delta ratio is smoothed by Gaussian smoothing window, with a window width of 8 s maximizing the correspondence to the results obtained using HPC recordings. Then, because the theta/delta ratio tends to be lower in the mPFC than in the hippocampus, the threshold to detect REM epochs is determined using the Otsu method (Otsu, 1979; which divides the theta/delta values into two groups maximizing inter-class variance) rather than the hard-coded threshold of 1 used for HPC recordings. The resulting REM periods thus obtained by PFC recordings matched the ones estimated by HPC recordings 93.45% of the time (**Supplementary Figure 3**).

4.2.2.3. Quiet Wakefulness Detection

Animals don't fall asleep in their freezing posture: at the minimum, they would always readjust their heads and more typically also curl up their bodies. This means that freezing and pre-sleep immobility are interrupted by movement. Therefore, other periods of immobility which preceded SWS by < 2 min were classified as immobile wakefulness. This duration is a parameter free to user selection, and reasonable choices would fall within a range of 30 s to a few minutes.

4.2.2.4. Freezing Detection

All the remaining immobility was classified as freezing with a minimum duration of freezing bouts and minimal interruptions set respectively to 2 and 0.2 s. These parameters are free to user selection in our code.

4.2.3. Analyses of Scoring Performance and Data Visualization

To assess the optimal smoothing window of the spindle power, we computed the effectiveness metric m of the k-means separation

of the smoothed spindle power in two groups, as defined by the proportion of inter-group variance and computed as $m = 1 - \frac{\sigma_i}{\sigma_{tot}}$, where σ_i is the intra-group variance σ_{tot} is the total variance of the smoothed spindle power.

To compute spectrograms, we employed an adapted version of the wavelet transform code from <http://paos.colorado.edu/research/wavelets/>.

CODE AVAILABILITY STATEMENT

A Matlab function to apply the scoring pipeline presented here is freely available on github (<https://github.com/mnpompili/behavioralStates.git>).

DATA AVAILABILITY STATEMENT

The data supporting the conclusions of this article will be made available by the authors upon request.

ETHICS STATEMENT

The animal protocol was reviewed and approved by Comité d’Ethique en Matière d’Expérimentation Animale N°59.

AUTHOR CONTRIBUTIONS

MP and RT: research project conception and design and data analysis. MP: funding gathering and project management. RT: algorithm conception and implementation. MP with contributions from RT: manuscript. Both authors contributed to the article and approved the submitted version.

FUNDING

MP was supported by the Agence Nationale de la Recherche (ANR-20-NEUC-0005-01) and RT by Cornell University.

REFERENCES

- Bagur, S., Lacroix, M. M., de Lavilléon, G., Lefort, J. M., Geoffroy, H., and Benchenane, K. (2018). Harnessing olfactory bulb oscillations to perform fully brain-based sleep-scoring and real-time monitoring of anaesthesia depth. *PLoS Biol.* 16:e2005458. doi: 10.1371/journal.pbio.2005458
- Bagur, S., Lefort, J. M., Lacroix, M. M., de Lavilléon, G., Herry, C., Chouvaeff, M., et al. (2021). Breathing-driven prefrontal oscillations regulate maintenance of conditioned-fear evoked freezing independently of initiation. *Nat. Commun.* 12, 1–15. doi: 10.1038/s41467-021-22798-6
- Benchenane, K., Peyrache, A., Khamassi, M., Tierney, P. L., Gioanni, Y., Battaglia, F. P., et al. (2010). Coherent theta oscillations and reorganization of spike timing in the hippocampal- prefrontal network upon learning. *Neuron* 66, 921–936. doi: 10.1016/j.neuron.2010.05.013
- Biskamp, J., Bartos, M., and Sauer, J. F. (2017). Organization of prefrontal network activity by respiration-related oscillations. *Sci. Rep.* 7, 1–11. doi: 10.1038/srep45508
- Blanchard, R. J., and Blanchard, D. C. (1969). Crouching as an index of fear. *J. Compar. Physiol. Psychol.* 67, 370–375. doi: 10.1037/h0026779

ACKNOWLEDGMENTS

We thank Sidney Wiener, Michaël Zugaro, and Christophe Bernard for help hosting and financing this work.

SUPPLEMENTARY MATERIAL

The Supplementary Material for this article can be found online at: <https://www.frontiersin.org/articles/10.3389/fncir.2022.783768/full#supplementary-material>

Supplementary Video 1 | Representative video of a rat sleeping in the resting environment. The video corresponds to the time interval shown on the left side of **Figure 1B**, part of the resting session immediately preceding the first contextual extinction session. Note how the animal sleeps almost all the time with small movements to adjust its posture.

Supplementary Video 2 | Representative video of a rat freezing in the conditioning environment. The video corresponds to the time interval shown on the right side of **Figure 1B**, that is the baseline period of the first contextual extinction session. These are the first moments the animal enters this environment since conditioning. Note how the animal freezes all the time in a stiff position and only the movements associated to a deep respiration are visible.

Supplementary Video 3 | Representative video of an animal exploring the conditioning environment. This corresponds to the first 30 seconds of exposure to the conditioning environment on the fourth day of extinction. This is the same rat of **Supplementary Video 2** but after 3 sessions of contextual fear extinction. Note how the animal does not freeze any more and explores the environment as the contextual fear has been extinguished.

Supplementary Video 4 | Representative video of an animal sleeping in the conditioning environment. This corresponds to 30 seconds in the conditioning environment on the fourth day of extinction. Namely, the same session of **Supplementary Video 3** 15 minutes later. Note how the animal sleeps, although uncomfortably, on the rods of the floor. The reclined head adjusted on the fore-paws is a good sleep marker.

Supplementary Video 5 | Video corresponding to the example session of **Figure 3F** where both freezing and sleeping were detected. The timestamp overlaid on video frames are on the same time scale of the x axis of the figure. Note how the animal explores the environment during baseline, freezes after the onsets of the first two CS+ presentations, but then gradually falls asleep. This rest is systematically interrupted by CS+ presentations (only two episodes shown in this video). All these transitions were captured by our technique as shown in **Figure 3F**.

- Brankack, J., Kukushka, V. I., Vyssotski, A. L., and Draguhn, A. (2010). EEG gamma frequency and sleep-wake scoring in mice: comparing two types of supervised classifiers. *Brain Res.* 1322, 59–71. doi: 10.1016/j.brainres.2010.01.069
- Buzsáki, G., Peyrache, A., and Kubie, J. (2014). Emergence of cognition from action. *Cold Spring Harb. Symp. Quant. Biol.* 79, 41–50. doi: 10.1101/sqb.2014.79.024679
- Chung, J. E., Joo, H. R., Fan, J. L., Liu, D. F., Barnett, A. H., Chen, S., et al. (2019). High-density, long-lasting, and multi-region electrophysiological recordings using polymer electrode arrays. *Neuron* 101, 21–31.e5. doi: 10.1016/j.neuron.2018.11.002
- Ciatipis, M., Branka, K. J., Draguhn, A., Tort, A. B. L., and Yanovsky, Y. (2014). Slow oscillations in the mouse hippocampus entrained by nasal respiration. *J. Neurosci.* 34, 5949–5964. doi: 10.1523/JNEUROSCI.5287-13.2014
- Courtin, J., Chaudun, F., Rozeske, R. R., Karalis, N., Gonzalez-Campo, C., Wurtz, H., et al. (2014). Prefrontal parvalbumin interneurons shape neuronal activity to drive fear expression. *Nature* 505, 92–96. doi: 10.1038/nature12755
- Datta, S., and Hobson, J. A. (2000). The rat as an experimental model for sleep neurophysiology. *Behav. Neurosci.* 114, 1239–1244. doi: 10.1037/0735-7044.114.6.1239

- Dhawale, A. K., Poddar, R., Wolff, S. B., Normand, V. A., Kopelowitz, E., and Ölveczky, B. P. (2017). Automated long-term recording and analysis of neural activity in behaving animals. *eLife* 6, 1–40. doi: 10.7554/eLife.27702
- Drieu, C., Todorova, R., and Zugaro, M. (2018). Nested sequences of hippocampal assemblies during behavior support subsequent sleep replay. *Science* 362, 675–679. doi: 10.1126/science.aat2952
- Fanselow, M. S., and Poulos, A. M. (2005). The neuroscience of mammalian associative learning. *Annu. Rev. Psychol.* 56, 207–234. doi: 10.1146/annurev.psych.56.091103.070213
- Fernandez, L. M., and Lüthi, A. (2020). Sleep spindles: mechanisms and functions. *Physiol. Rev.* 100, 805–868. doi: 10.1152/physrev.00042.2018
- Girardeau, G., Inema, I., and Buzsáki, G. (2017). Reactivations of emotional memory in the hippocampus/amygdala system during sleep. *Nat. Neurosci.* 20:1634. doi: 10.1038/nn.4637
- Gottesmann, C., de Mendoza, J. L. J., Lacoste, G., Lallement, B., Rodrigues, L., and Tasset, M. (1971). Etude sur l'analyse et la quantification automatiques del différents états de veille et de sommeil chez le Rat. *CR Acad. Sci.* 272, 301–302.
- Gottesmann, C., Kirkham, P. A., Lacoste, G., Rodrigues, L., and Arnaud, C. (1977). Automatic analysis of the sleep-waking cycle in the rat recorded by miniature telemetry. *Brain Res.* 132, 562–568. doi: 10.1016/0006-8993(77)90205-0
- Gründemann, J., Bitterman, Y., Lu, T., Krabbe, S., Grewe, B. F., Schnitzer, M. J., et al. (2019). Amygdala ensembles encode behavioral states. *Science* 364:aav8736. doi: 10.1126/science.aav8736
- Hazan, L., Zugaro, M., and Buzsáki, G. (2006). Klusters, NeuroScope, NDManager: a free software suite for neurophysiological data processing and visualization. *J. Neurosci. Methods* 155, 207–216. doi: 10.1016/j.jneumeth.2006.01.017
- Hengen, K. B., Torrado Pacheco, A., McGregor, J. N., Van Hooser, S. D., and Turrigiano, G. G. (2016). Neuronal firing rate homeostasis is inhibited by sleep and promoted by wake. *Cell* 165, 180–191. doi: 10.1016/j.cell.2016.01.046
- Herent, C., Diem, S., Fortin, G., and Bouvier, J. (2020). Absent phasing of respiratory and locomotor rhythms in running mice. *eLife* 9, 1–21. doi: 10.7554/eLife.61919
- Hirase, H., Leinekugel, X., Czurkó, A., Csicsvari, J., and Buzsáki, G. (2001). Firing rates of hippocampal neurons are preserved during subsequent sleep episodes and modified by novel awake experience. *Proc. Natl. Acad. Sci. U.S.A.* 98, 9386–9390. doi: 10.1073/pnas.161274398
- Jercog, D., Winke, N., Sung, K., Fernandez, M. M., Francioni, C., Rajot, D., et al. (2021). Dynamical prefrontal population coding during defensive behaviours. *Nature* 595, 690–694. doi: 10.1038/s41586-021-03726-6
- Johns, T. G., Piper, D. C., James, G. W., Birtley, R. D., and Fischer, M. (1977). Automated analysis of sleep in the rat. *Electroencephalogr. Clin. Neurophysiol.* 43, 103–105. doi: 10.1016/0013-4694(77)90201-2
- Karalis, N., Dejean, C., Chaudun, F., Khoder, S., Rozeske, R. R., Wurtz, H. H. H., et al. (2016). 4-Hz oscillations synchronize prefrontal-amygdala circuits during fear behavior. *Nat. Neurosci.* 19, 605–612. doi: 10.1038/nn.4251
- Karalis, N., and Sirota, A. (2022). Breathing coordinates cortico-hippocampal dynamics in mice during offline states. *Nat. Commun.* 13, 1–20. doi: 10.1038/s41467-022-28090-5
- Kohn, M., Litchfield, D., Branchey, M., and Brebbia, D. R. (1974). An automatic hybrid analyzer of sleep stages in the rat. *Electroencephalogr. Clin. Neurophysiol.* 37, 518–520. doi: 10.1016/0013-4694(74)90095-9
- Krakauer, J. W., Ghazanfar, A. A., Gomez-Marín, A., MacIver, M. A., and Poeppel, D. (2017). Neuroscience needs behavior: correcting a reductionist bias. *Neuron* 93, 480–490. doi: 10.1016/j.neuron.2016.12.041
- Liang, S. -F., Kuo, C. -E., Hu, Y. -H., and Cheng, Y. -S. (2012). A rule-based automatic sleep staging method. *J. Neurosci. Methods* 205, 169–176. doi: 10.1016/j.jneumeth.2011.12.022
- Lin, S. C., Gervasoni, D., and Nicolelis, M. A. (2006). Fast modulation of prefrontal cortex activity by basal forebrain noncholinergic neuronal ensembles. *J. Neurophysiol.* 96, 3209–3219. doi: 10.1152/jn.00524.2006
- Lockmann, A. L. V., Laplagne, D. A., Le ao, R. N., and Tort, A. B. L. (2016). A respiration-coupled rhythm in the rat hippocampus independent of theta and slow oscillations. *J. Neurosci.* 36, 5338–5352. doi: 10.1523/JNEUROSCI.3452-15.2016
- Louis, R. P., Lee, J., and Stephenson, R. (2004). Design and validation of a computer-based sleep-scoring algorithm. *J. Neurosci. Methods* 133, 71–80. doi: 10.1016/j.jneumeth.2003.09.025
- McCarley, R. W. (2007). Neurobiology of REM and NREM sleep. *Sleep Med.* 8, 302–330. doi: 10.1016/j.sleep.2007.03.005
- Moberly, A. H., Schreck, M., Bhattarai, J. P., Zweifel, L. S., Luo, W., and Ma, M. (2018). Olfactory inputs modulate respiration-related rhythmic activity in the prefrontal cortex and freezing behavior. *Nat. Commun.* 9, 1528. doi: 10.1038/s41467-018-03988-1
- Otsu, N. (1979). A threshold selection method from gray-level histograms. *IEEE Trans. Syst. Man Cybern.* 9, 62–66. doi: 10.1109/TSMC.1979.4310076
- Pasquet, M. O., Tihy, M., Gourgeon, A., Pompili, M. N., Godsil, B. P., Léna, C., et al. (2016). Wireless inertial measurement of head kinematics in freely-moving rats. *Sci. Rep.* 6:35689. doi: 10.1038/srep35689
- Paxinos, G., and Watson, C. (2013). *The Rat Brain in Stereotaxic Coordinate, 7th Edn.* New York, NY: Academic Press.
- Ressler, R. L., Goode, T. D., Kim, S., Ramanathan, K. R., and Maren, S. (2021). Covert capture and attenuation of a hippocampus-dependent fear memory. *Nat. Neurosci.* 24, 677–684. doi: 10.1038/s41593-021-00825-5
- Sosa, M., Joo, H. R., and Frank, L. M. (2020). Dorsal and ventral hippocampal sharp-wave ripples activate distinct nucleus accumbens networks. *Neuron* 105, 725–741.e8. doi: 10.1016/j.neuron.2019.11.022
- Steriade, M., McCormick, D. A., and Sejnowski, T. J. (1993). Thalamocortical oscillations in the sleeping and aroused brain. *Science* 262, 679–685. doi: 10.1126/science.8235588
- Supratak, A., Dong, H., Wu, C., and Guo, Y. (2017). DeepSleepNet: a model for automatic sleep stage scoring based on raw single-channel EEG. *IEEE Trans. Neural Syst. Rehabil. Eng.* 25, 1998–2008. doi: 10.1109/TNSRE.2017.2721116
- Tingley, D., McClain, K., Kaya, E., Carpenter, J., and Buzsáki, G. (2021). A metabolic function of the hippocampal sharp wave-ripple. *Nature* 597, 82–86. doi: 10.1038/s41586-021-03811-w
- Todorova, R., and Zugaro, M. B. (2019). Isolated cortical computations during delta waves. *Science* 366, 377–381. doi: 10.1126/science.aay0616
- Trouche, S., Pompili, M. N., and Girardeau, G. (2020). The role of sleep in emotional processing: insights and unknowns from rodent research. *Curr. Opin. Physiol.* 15, 230–237. doi: 10.1016/j.cophys.2020.04.003
- Wang, M., Foster, D. J., and Pfeiffer, B. E. (2020). Alternating sequences of future and past behavior encoded within hippocampal theta oscillations. *Science* 370, 247–250. doi: 10.1126/science.abb4151
- Wilson, M. A., and McNaughton, B. L. (1994). Reactivation of hippocampal ensemble memories during sleep. *Science* 265, 676–679. doi: 10.1126/science.8036517

Conflict of Interest: The authors declare that the research was conducted in the absence of any commercial or financial relationships that could be construed as a potential conflict of interest.

The handling editor declared past co-authorships with both authors.

Publisher's Note: All claims expressed in this article are solely those of the authors and do not necessarily represent those of their affiliated organizations, or those of the publisher, the editors and the reviewers. Any product that may be evaluated in this article, or claim that may be made by its manufacturer, is not guaranteed or endorsed by the publisher.

Copyright © 2022 Pompili and Todorova. This is an open-access article distributed under the terms of the Creative Commons Attribution License (CC BY). The use, distribution or reproduction in other forums is permitted, provided the original author(s) and the copyright owner(s) are credited and that the original publication in this journal is cited, in accordance with accepted academic practice. No use, distribution or reproduction is permitted which does not comply with these terms.